universe

MDPI

Article

Weak Deflection Angle and Shadow by Tidal Charged Black Hole

Wajiha Javed [1], Ali Hamza [1] and Ali Övgün [2,*]

[1] Division of Science and Technology, University of Education, Township Campus, Lahore 54590, Pakistan; wajiha.javed@ue.edu.pk (W.J.); msf1800077@ue.edu.pk (A.H.)
[2] Physics Department, Eastern Mediterranean University, North Cyprus via Mersin 10, 99628 Famagusta, Turkey
* Correspondence: ali.ovgun@emu.edu.tr

Abstract: In this article, we calculate the deflection angle of a tidal charged black hole (TCBH) in weak field limits. First, we obtain the Gaussian optical curvature and then apply the Gauss–Bonnet theorem on it. With the help of Gibbons–Werner method, we are able to calculate the light's deflection angle by TCBH in weak field limits. After calculating the deflection angle of light, we check the graphical behavior of TCBH. Moreover, we further find the light's deflection angle in the presence of the plasma medium and also check the graphical behavior in the presence of the plasma medium. Moreover, we investigate the shadow of TCBH. For calculating the shadow, we first find the null geodesics around the TCBH and then find its shadow radius. We also obtain TCBH's shadow in the plasma medium. Hence, we discuss the shadow of the TCBH, using the $M87^*$ parameters announced by the event horizon telescope.

Keywords: relativity; gravitation; black hole; tidal charge; Gauss–Bonnet theorem; plasma medium; shadow

PACS: 95.30.Sf; 98.62.Sb; 97.60.Lf

Citation: Javed, W.; Hamza, A.; Övgün, A. Weak Deflection Angle and Shadow by Tidal Charged Black Hole. *Universe* **2021**, *7*, 385. https://doi.org/10.3390/universe7100385

Academic Editor: Lorenzo Iorio

Received: 21 September 2021
Accepted: 12 October 2021
Published: 18 October 2021

1. Introduction

Einstein's theory of general relativity (GR) is a gravity theory which was developed in 1916. Einstein anticipated the presence of gravitational waves and gravitational lensing in his theory of GR [1]. Black holes (BHs) are captivating objects in the universe. It is assumed that various types of BHs live in the universe; this was experimentally confirmed by the laser interferometer gravitational-wave observatory (LIGO) experiment in 2015 [2]. After that, EHT collaboration showed the existence of the black hole by its shadow in 2019 [3]. BH physics is very important because it plays a vital role in the discovery of the gravitational wave [2]; furthermore, BH physics is used for understanding entropy and the information paradox [4]. It is also used in an interesting aspect of gravitational lensing. As indicated by Einstein, light bends around a massive object, such as a black hole, causing it to act as a lens for the things that lie behind it. Strong lensing generates curves and rings, for example, Einstein's ring, while weak lensing gravity does not create the image of a distant galaxy, but it still produces a measurable useful effect. Moreover, weak lensing provides an independent measurement of dark energy, the substance causing the accelerated expansion of the universe.

Gravitational lensing is a useful system to comprehend the galaxies, dark matter of the universe, dark energy and the universe [5]. As the main gravitational lensing perception by the Eddington, a huge work on gravitational lensing was accomplished for black holes, wormholes, cosmic strings and various types of spacetimes [6–26]. Since Einstein, the geodesic technique [27–32] has been considered for investigating the gravitational lensing. In 2008, Gibbons and Werner showed a new way to calculate the weak deflection angle

by introducing the Gauss–Bonnet theorem (GBT) [33]. Using GBT, they found light's weak gravitational deflection in the static and spherically symmetric (SSS) spacetime, e.g., Schwarzschild spacetime [33]. Then, Werner showed that it is also possible to find the weak deflection angle of stationary black holes, such as the Kerr black hole, using GBT [34]. In GBT, the light's deflection angle can be determined by integrating the Gaussian curvature of related optical metrics. In GBT, we can utilize a space D_R, which is limited by the photon beam, just as a circular boundary curve that is situated at the focal point and photon beams that meet the source and observer. It is expected that both the origin and observer are at the coordinate distance R from the focal point. The GBT is written as follows [33]:

$$\int\int_{D_R} \mathcal{K} dS + \oint_{\partial D_R} \kappa \, dt + \Sigma_i \theta_i = 2\pi \mathcal{X}(D_R).$$

Here, the optical Gaussian curvature is denoted by $\mathcal{K}$ and an areal component is denoted by dS. Subsequently, thinking about the Euler characteristic, $\mathcal{X}(D_R) = 1$, the jump angles are $\Sigma_i \theta_i = \pi$, by using straight light approximation and GBT. Then, the weak deflection angle is calculated as follows [33]:

$$\alpha = -\int_0^{\pi} \int_{\frac{b}{r \sin \phi}}^{\infty} \mathcal{K} dS.$$

Note that the deflection angle is denoted by α. The weak deflection angle, using the GBT for various spacetimes, was studied by many physicists. For example, the deflection angle of light was studied for BHs and wormholes by the following authors [35–53]: Ovgun et al. studied for different spacetimes, such as Schwarzschild-like spacetime, the bumblebee gravity model [54–60], and Javed et al. studied the impact of various matter fields [61–65]. Next, Ishihara et al. [66] showed that it is conceivable to calculate the weak deflection angle using the finite-distances method. Moreover, Ono et al. [67] extended the method to stationary axisymmetric spacetimes. The strong deflection angle for finite distance was discussed by Ishihara et al. [68]. After that, Crisnejo and Gallo [69] and many other authors [70–90] contemplated the light's deflection angle in the presence of a plasma medium.

Most of the scientists have said that supermassive BHs exist at the center of the Milky Way galaxy and they hope to detect its shadow. Additionally, the new results can provide physicists with an unprecedented look at black hole dynamics that will enable scientists to test general relativity [3–102]. Some say that what we call a shadow is a dark interior with a bright ring of radiation emitted by fast-moving, superheated gas swirling around, and falling into, the black hole. The shadow of a black hole is caused by gravitational light deflection. The trajectory of a photon in vacuum is determined by its impact parameter. The photon sphere plays a crucial role in the formation of the shadow. The size of the shadow radius for the black hole at the center of the Milky Way galaxy is about 53 μas. The shadow of the stationary black hole is deformed and oblate, while the shadow of the non-rotating black hole is just a circle. There are various types of scientific studies on black hole shadow in the literature. For example, the shadow for negative tidal charges and charges corresponding to naked singularities are also discussed in [11]. Moreover, Zakharov has studied constraints on a charge in the Reissner–Nordström metric for the black hole at the Galactic Center [11], and then has showed constraints on the tidal charge of the supermassive black hole at the Galactic Center with trajectories of bright stars [12]. Neves also has studied constraining the tidal charge of brane black holes, using their shadows [14]. Recently, Kocherlakota et al. presented constraints on black hole charge from observations of $M87^*$ in 2017 [91], where the authors used the dependence of the shadow size on the black hole charge for the Reissner–Nordstrom metric. It was shown that the shadow size decreases with increasing the charge [13,91]. Based on the results of the shadow evaluation for $M87^*$ performed by the EHT team, Zakharov constrained a

tidal charge $q > -1.22$ and evaluated a tidal charge of $q > -0.25$ from the shadow size estimates for $SgrA^*$ in [13].

The paper is organized as follows: in Section 2, we derive the optical metric for the TCBH and find the weak deflection angle, using the GBT in Section 3. In Section 4, we discuss the graphical behavior and find the weak deflection angle in the presence of the plasma medium, using the GBT in Section 5. Next, we find the graphical behavior in the presence of plasma in Section 6 and calculate the null geodesics of the TCBH in Section 7. Further, we calculate the shadow of the TCBH in Section 8 and also calculate the shadow of the TCBH in the presence of plasma in Section 9. Finally, we conclude our results in Section 10.

2. Optical Metric of TCBH

The line element of a SSS TCBH is given by the following [103,104]:

$$ds^2 = -B(r)dt^2 + \frac{dr^2}{B(r)} + r^2 d\Omega_2^2, \tag{1}$$

where

$$B(r) = 1 - \frac{2M}{M_p^2 r} + \frac{q}{M_5^2 r^2}, \tag{2}$$

and

$$d\Omega_2^2 = d\theta^2 + \sin^2\theta d\phi^2, \tag{3}$$

Here, BH's mass is denoted by M; the dimensionless tidal charge is denoted by q; M_p(=1.2 $\times$ $10^{16} Tev$) denotes the effective Planck mass on the brane; and M_5 denotes the fundamental Planck scale in the 5D bulk. It is noted that, generally, $M_5 << M_p$.

By assuming the equatorial coordinate plane ($\theta = \frac{\pi}{2}$), we obtain the optical metric of TCBH as follows:

$$dt^2 = \frac{dr^2}{B^2(r)} + \frac{r^2 d\phi^2}{B(r)}. \tag{4}$$

Then, we calculate the Gaussian optical curvature as follows:

$$\mathcal{K} = \frac{RicciScalar}{2} \approx -\frac{-2M}{r^3 M_p^2} - \frac{6qM}{r^5 M_p^2 M_5^2} + \frac{3q}{r^4 M_5^2} + \mathcal{O}\left(M^2, q^2\right). \tag{5}$$

3. Deflection Angle of TCBH

In this section, we find the deflection angle by TCBH with the help of GBT, which is written as follows [33]:

$$\int\int_{\mathcal{F}_T} \mathcal{K} dS + \oint_{\partial \mathcal{F}_T} k dt + \sum_l \epsilon_l = 2\pi \mathcal{Z}(\mathcal{F}_T), \tag{6}$$

Here, $\mathcal{K}$ denotes the Gaussian curvature, and k denotes the geodesic curvature as $k = \bar{g}(\nabla_{\dot{\beta}}\dot{\beta}, \ddot{\beta})$, where $\bar{g}(\dot{\beta}, \dot{\beta}) = 1$, $\ddot{\beta}$ shows the unit acceleration vector, and the ϵ_l shows the exterior angle at the lth vertex. Since $T \to \infty$, both of the jump angles become $\pi/2$ and then we have $\theta_O + \theta_T \to \pi$. The Euler characteristic is $\mathcal{Z}(\mathcal{F}_T) = 1$, as $\mathcal{F}_T$ is non singular. So, we have the following:

$$\int\int_{\mathcal{F}_T} \mathcal{K} dS + \oint_{\partial \mathcal{F}_T} k dt + \epsilon_l = 2\pi \mathcal{Z}(\mathcal{F}_T), \tag{7}$$

Here, $\epsilon_l = \pi$ demonstrates that both $\alpha_{\bar{g}}$ and the total jump angles are geodesic, and $\mathcal{Z}$ is the Euler characteristic number and it is equal to 1. As $T \to \infty$, then we have $k(E_T) = |\nabla_{\dot{E}_T} \dot{E}_{ST}|$. The radial component of the geodesic curvature is written as follows [33]:

$$(\nabla_{\dot{E}_T} \dot{E}_T)^r = \dot{E}_T^{\phi} \partial_{\phi} \dot{E}_T^r + \Gamma_{11}^0 (\dot{E}_T^{\phi})^2. \tag{8}$$

for large T, $E_T := r(\phi) = T = const$. Hence, Equation (8) becomes $(\dot{E}_T^{\phi})^2 = \frac{A^2(r)B(r)}{r^2}$. As $\Gamma^0_{11} = -rB + \frac{r^2B'(r)}{2}$, it becomes the following:

$$(\nabla_{\dot{E}_T^r}\dot{E}_T^r)^r \to \frac{1}{T}, \tag{9}$$

so that $k(E_T) \to T^{-1}$. By using the optical metric Equation (4) and writing it as $dt = Td\phi$, we have $k(E_T)dt = d\phi$.

By combining all the results, we have the following:

$$\int\int_{\mathcal{F}_T} \mathcal{K}ds + \oint_{\partial\mathcal{F}_T} kdt =^{T\to\infty} \int\int_{U_\infty} \mathcal{K}dS + \int_0^{\pi+\Theta} d\phi. \tag{10}$$

The light ray in weak field limits at the zeroth order (straight light approximation) is written as $r(t) = b/\sin\phi$. Using the above steps, the weak deflection angle can be calculated by the following [33]:

$$\Theta = -\int_0^{\pi}\int_{b/\sin\phi}^{\infty} \mathcal{K}\sqrt{det\bar{g}}\, drd\phi, \tag{11}$$

Here, $\sqrt{det\bar{g}} \approx rdr$.

After replacing the Gaussian optical curvature Equation (5) into Equation (11), the weak deflection angle is obtained as follows:

$$\Theta \approx \frac{4M}{bM_p^2} - \frac{3q\pi}{4b^2M_5^2} + \mathcal{O}(M^2, q^2). \tag{12}$$

On the other hand, the deflection angle of the Reissner–Nordstrom (RN) BH in [105] is given as follows:

$$\Theta_{RNBH} \approx \frac{4M}{b} + \frac{15\pi M^2}{4b^2} - \frac{3q^2\pi M^2}{4b^2} + \mathcal{O}(M^3, b^3). \tag{13}$$

Note that increasing the value of tidal charge decreases the deflection angle. We compare these results in the graphical section.

4. Graphical Analysis for Non-Plasma Medium

In this section, we obtain the graphical behavior of TCBH's deflection angle. We check the graphical behavior in correspondence of deflection angle Θ with impact parameter b by varying the value of dimensionless tidal charge q.

Figures 1 and 2 demonstrate the relation of Θ w.r.t b for different values of q of TCBH. We observe that the deflection angle continuously decreases with increasing q and shows a constant behavior.

By comparing the graphs of RNBH and TCBH, we observe that deflection angle of RN is larger than the deflection angle of TCBH. We conclude that the tidal charge decreases the deflection angle as compared with the RN charge in Figures 1 and 2.

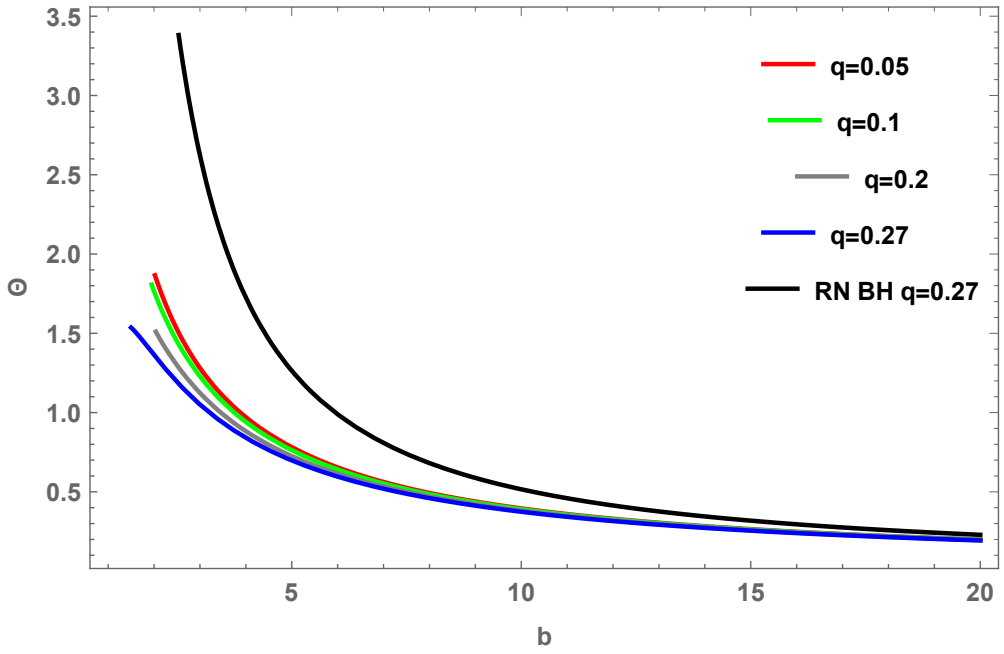

Figure 1. Relation between Θ and b of TCBH for positive values of q for $M_p = 1$, $M_5 = 0.5$, $M = 1$.

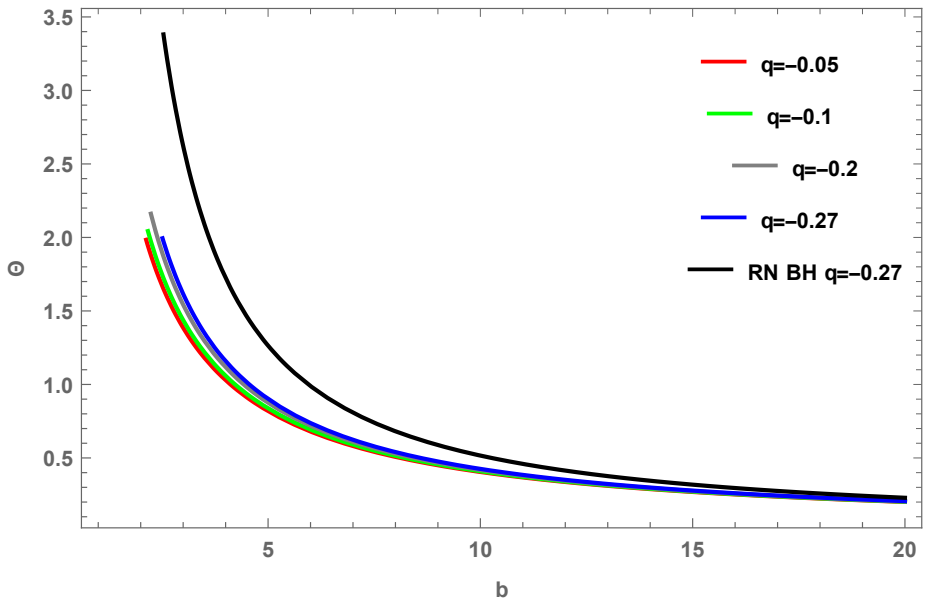

Figure 2. Relation between Θ and b of TCBH for negative values of q for $M_p = 1$, $M_5 = 0.5$, $M = 1$.

5. Effect of Plasma on Gravitational Lensing

In this section, we check how a plasma medium affects the gravitational lensing of TCBH. Now, we assume that the TCBH in the presence of plasma is illustrated by the refractive index n [76,77]:

$$n^2(r, \omega(r)) = 1 - \frac{\omega_e^2(r)}{\omega^2(r)}. \tag{14}$$

Here, the refractive index is defined as follows:

$$n(r) = \sqrt{1 - \frac{\omega_e^2}{\omega_\infty^2}\left(1 - \frac{2M}{M_p^2 r} + \frac{q}{M_5^2 r^2}\right)}, \tag{15}$$

where $\omega(r)$ is the photon frequency and $\omega_e(r)$ is the electron plasma frequency and ω_e is considered the homogeneous plasma.

The optical metric of Equation (1) in plasma medium is written as follows [69]:

$$dt^2 = g^{opt}_{lm} dx^l dx^m = n^2 \left[\frac{dr^2}{B^2(r)} + \frac{r^2 d\phi^2}{B(r)} \right], \tag{16}$$

with determinant g^{opt}_{lm} as follows:

$$\sqrt{g^{opt}} = r(1 - \frac{\omega_e^2}{\omega_\infty^2}) + \frac{M}{M_p^2(r)}(3 + \frac{\omega_e^2}{\omega_\infty^2}) - \frac{q}{2M_5^2 r}(3 + \frac{\omega_e^2}{\omega_\infty^2}). \tag{17}$$

Then, the optical Gaussian curvature can be calculated by the following:

$$\mathcal{K} = -3\frac{M{\omega_e}^2}{r^3{\omega_\infty}^2{M_p}^2} - 2\frac{M}{{M_p}^2 r^3} + 5\frac{q{\omega_e}^2}{{\omega_\infty}^2 M_5^2 r^4} + 3\frac{q}{M_5^2 r^4} - 26\frac{qM{\omega_e}^2}{{\omega_\infty}^2 M_5^2 {M_p}^2 r^5} - 6\frac{qM}{M_5^2 {M_p}^2 r^5}. \tag{18}$$

With the help of GBT, we obtain the deflection angle of TCBH in the presence of the plasma medium. So, for obtaining deflection angle in weak field limit, we apply the condition of $r = \frac{b}{sin\phi}$ at the 0th order:

$$\Theta = -\lim_{R\to 0} \int_0^\pi \int_{\frac{b}{\sin\phi}}^R \mathcal{K} dS, \tag{19}$$

Using the above equation with the optical Gaussian curvature, the deflection angle of light in the presence of the plasma medium is found as follows:

$$\Theta = 4\frac{M}{b{M_p}^2} + 3/4\frac{q{\omega_e}^2\pi}{b^2{\omega_\infty}^2{M_5}^2} - 3/4\frac{q\pi}{b^2{M_5}^2} - 6\frac{M{\omega_e}^2}{b{\omega_\infty}^2{M_p}^2} + \mathcal{O}(M^2, q^2, \frac{\omega_e^3}{\omega_\infty^3}). \tag{20}$$

Note that one can neglect the plasma medium effect by $(\frac{\omega_e}{\omega_\infty} \to 0)$; then, this deflection angle in Equation (20) reduces into the angle in Equation (13).

6. Graphical Analysis for Plasma Medium

Here, for simplicity, we take $\frac{\omega_e}{\omega_\infty} = 10^{-1}$ and observe the deflection angle by changing the value of the dimensionless tidal charge q.

Figure 3 demonstrates the relation of Θ with b for different values of q in the plasma medium. In this plot, we observe that increasing the value of q decreases the deflection angle in the plasma medium. Moreover, the deflection angle in the plasma medium is smaller than the deflection angle in the vacuum.

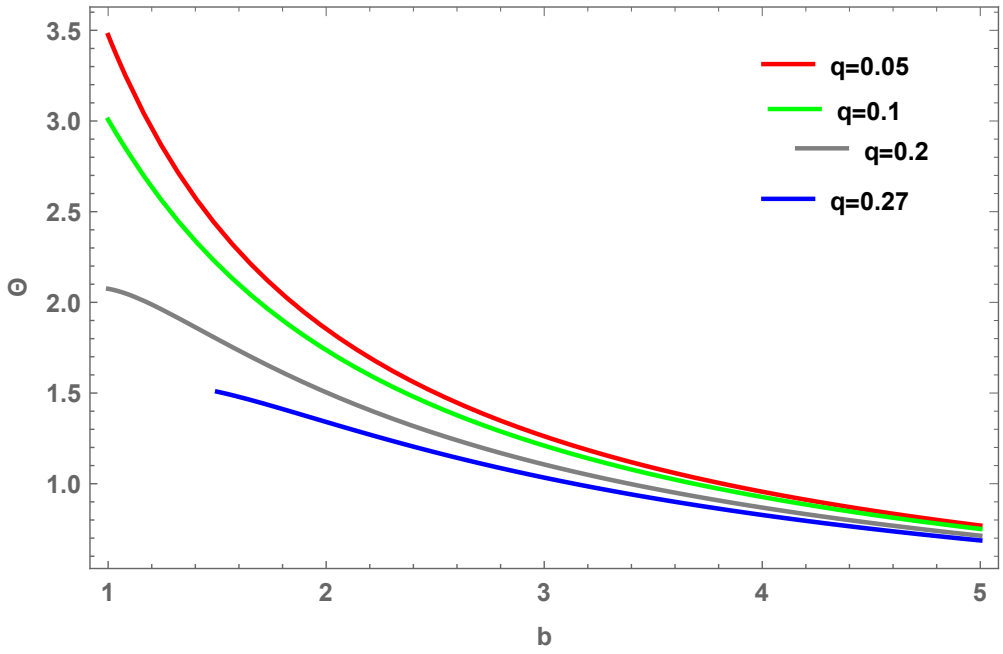

Figure 3. Relation between Θ and b of tidal-charged BH for positive values of q for $M_p = 1$, $M_5 = 0.5$, $M = 1$ and $\frac{\omega_e}{\omega_\infty} = 10^{-1}$ for exaggeration of the plot.

7. Null Geodesic in a TCBH

The Lagrangian representing the motion of light in the TCBH's spacetime using Equation (1) is written as follows:

$$2\mathcal{L} = -\left(1 - \frac{2M}{M_p^2 r} + \frac{q}{M_5^2 r^2}\right)\dot{t}^2 + \left(1 - \frac{2M}{M_p^2 r} + \frac{q}{M_5^2 r^2}\right)\dot{r}^2 + r^2\dot{\theta}^2 + r^2\sin^2\theta\dot{\phi}^2, \tag{21}$$

Here, the derivative w.r.t the affine parameter λ is represented by an overdot. As the Lagrangian is not dependent on it and ϕ, we introduce two new constants named energy E and the angular momentum L, where the values of these constants are defined as follows:

$$p_t = \frac{\partial L}{\partial \dot{t}} = -(1 - \frac{2M}{M_p^2 r} + \frac{q}{M_5^2 r^2})\dot{t} = -E, \tag{22}$$

and

$$p_\phi = \frac{\partial L}{\partial \dot{\phi}} = r^2\sin^2\theta\dot{\phi} = L. \tag{23}$$

For finding the restrictions of the geodesic, we use these constants as follows:

$$\frac{dt}{d\lambda} = \dot{t} = \frac{E}{1 - \frac{2M}{M_p^2 r} + \frac{q}{M_5^2 r^2}} \quad , \quad \frac{d\phi}{d\lambda} = \dot{\phi} = \frac{L}{r^2\sin^2\theta}. \tag{24}$$

Now, we define the new parts of the momentum named the r-part and θ-part:

$$p_r = \frac{\partial L}{\partial \dot{r}} = \frac{\dot{r}}{1 - \frac{2M}{M_p^2 r} + \frac{q}{M_5^2 r^2}} \quad and \quad p_\theta = \frac{\partial L}{\partial \dot{\theta}} = r^2\dot{\theta}. \tag{25}$$

With the help of the Hamilton–Jacobi equation, we find the values of the r-part and θ-part of the geodesic equation as follows:

$$\frac{\partial S}{\partial \lambda} = -\frac{1}{2}g^{\mu\nu}\frac{\partial S}{\partial x^\mu}\frac{\partial S}{\partial x^\nu}, \tag{26}$$

and for photons ($m_0 = 0$), Equation (26) can give us the result of the following type:

$$S = -Et + L\phi + S_r(r) + S_\theta(\theta), \tag{27}$$

where S_r depends on r, and S_θ depends on θ. Now, we obtain the Carter constant ($\pm\mathcal{K}$) [100] by separating the values of r and θ. We obtain these values of r and θ by replacing Equation (27) into Equation (26). By substituting the values of the contravariant metric, i.e., $g^{\mu\nu}$, we have the following:

$$\frac{1}{\sqrt{1 - \frac{2M}{M_p^2 r} + \frac{q}{M_5^2 r^2}}} \frac{dr}{d\lambda} =^{+}_{-} \sqrt{R}(r),$$
$$r^2 \frac{d\theta}{d\lambda} =^{+}_{-} \sqrt{T}(\theta), \tag{28}$$

where the values of R and θ can be defined as follows:

$$R(r) = \frac{E^2}{1 - \frac{2M}{M_p^2 r} + \frac{q}{M_5^2 r^2}} - \frac{\mathcal{K}}{r^2},$$
$$T(\theta) = \mathcal{K} - \frac{L^2}{\sin^2\theta}. \tag{29}$$

Now, Equation S_r can be written as follows:

$$\frac{dr}{d\lambda}^2 + V_{eff} = 0, \tag{30}$$

with

$$V_{eff} = -\left(1 - \frac{2M}{M_p^2 r} + \frac{q}{M_5^2 r^2}\right) R(r). \tag{31}$$

We see that the effective potential depends on BH's mass denoted by M, and the dimensionless tidal charge denoted by q and effective Planck mass on the brane denoted by M_p and fundamental Planck scale in the 5D bulk denoted by M_5 and radius r and $R(r)$. Now, we change these parameters to new impact parameters, such as $\xi = \frac{L}{E}$ and $\eta = \frac{\mathcal{K}}{E^2}$. Now, we change the value of R with respect to these new impact parameters.

$$R = E^2[\frac{1}{1 - \frac{2M}{M_p^2 r} + \frac{q}{M_5^2 r^2}} - \frac{\eta}{r^2}]. \tag{32}$$

8. Shadow of TCBH

Here, in this section, we find the shadow of TCBH and we discuss in detail about shadow in the introduction. Now, for finding the shadow, we find the unstable circular photons orbits [106]. For this, we must satisfy the following:

$$R = 0 \quad and \quad R' = 0, \tag{33}$$

where prime ($\prime$) means differentiation w.r.t r. Putting (32) into (33), we obtain the relation for the photon sphere as follows:

$$\frac{B'(r)}{B(r)} = \frac{2}{r}. \tag{34}$$

and the photon sphere r_p is derived as follows:

$$r_p = \frac{3M_5^2 M + \sqrt{9M_5^4 M^2 - 8M_5^2 M_p^4 q}}{2M_5^2 M_p^2}. \tag{35}$$

The radius of the shadow r_s at photon sphere radius r_p is calculated as follows:

$$r_s = \sqrt{\eta + \xi^2} = \frac{r_p}{\sqrt{1 - \frac{2M}{M_p^2 r_p} + \frac{q}{M_5^2 r_p^2}}}, \tag{36}$$

$$r_s = \frac{1}{2}\sqrt{\frac{\left(3M_5^2 M + \sqrt{9M_5 M_5^4 M^2 - 8M_5^2 M_p^4 q}\right)^3}{M_5^4 M_p^2\left(3M_5^2 M^2 + M\sqrt{9M_5^4 M^2 - 8M_5^2 M_p^4 q} - 2M_p^4 q\right)}}, \tag{37}$$

where the impact parameters depend on the BHs mass denoted by M, the dimensionless tidal charge denoted by q, effective Planck mass on the brane denoted by M_p, and fundamental Planck scale in the 5D bulk denoted by M_5. So Equation (36) provides detail about the boundary of the shadow. An observer that is far away from the BH can find this shadow in this sky and we make new coordinates in the observer's sky, named the celestial coordinates (α,β); we relate these coordinates with impact parameters (ξ,η). These coordinates are defined in these papers [101,102] as follows:

$$\begin{aligned} \alpha &= \lim_{r_0 \to \infty} (r_0^2 \sin\theta_0)\frac{d\phi}{dr}, \\ \beta &= \lim_{r_0 \to \infty} r_0^2 \frac{d\theta}{dr}. \end{aligned} \tag{38}$$

Note that r_0 represents the distance between the viewer and the BH, and θ_0 denotes the angular coordinates of the observer called the "inclination angle". After putting the equations of four velocities into Equation (38), and doing some calculations, we obtain these celestial coordinates as follows:

$$\alpha = -\frac{\xi}{\sin\theta_0} \qquad and \qquad \beta = \sqrt{\eta - \frac{\xi^2}{\sin\theta_0^2}}. \tag{39}$$

With the help of these equations and using the impact parameters, we now make the shape of the TCBH shadow. For plotting the shadows's shape, we plot α versus β, which gives details about the boundary of the TCBH in the observer's sky. These plots are seen in Table 1 and Figure 4.

We plot the shadow of the black hole by changing the values of the dimensionless tidal charge q, using the constraints from the astronomical observations on the upper limiting values on the tidal charge parameters [12,14]. In this plot, we also discuss the shadow for positive and negative values of q. We see that the shadow's shape is a perfect circle, and its shape is shown in Figure 4. In this graph, we see that for small values of q, the radius of the shadow shows a different behavior. Increasing the value of the tidal charge decreases the radius of the shadow as well as the radius of the photon sphere.

Table 1. Effects of the tidal charge on the BH shadow for fixed $M_p = 1$, $M_5 = 0.5$, $M = 1$.

q	r_p	R_s
0.05	2.86015	2.96572
0.1	2.70416	2.92949
0.2	2.30623	2.8537
0.27	1.8	2.84605

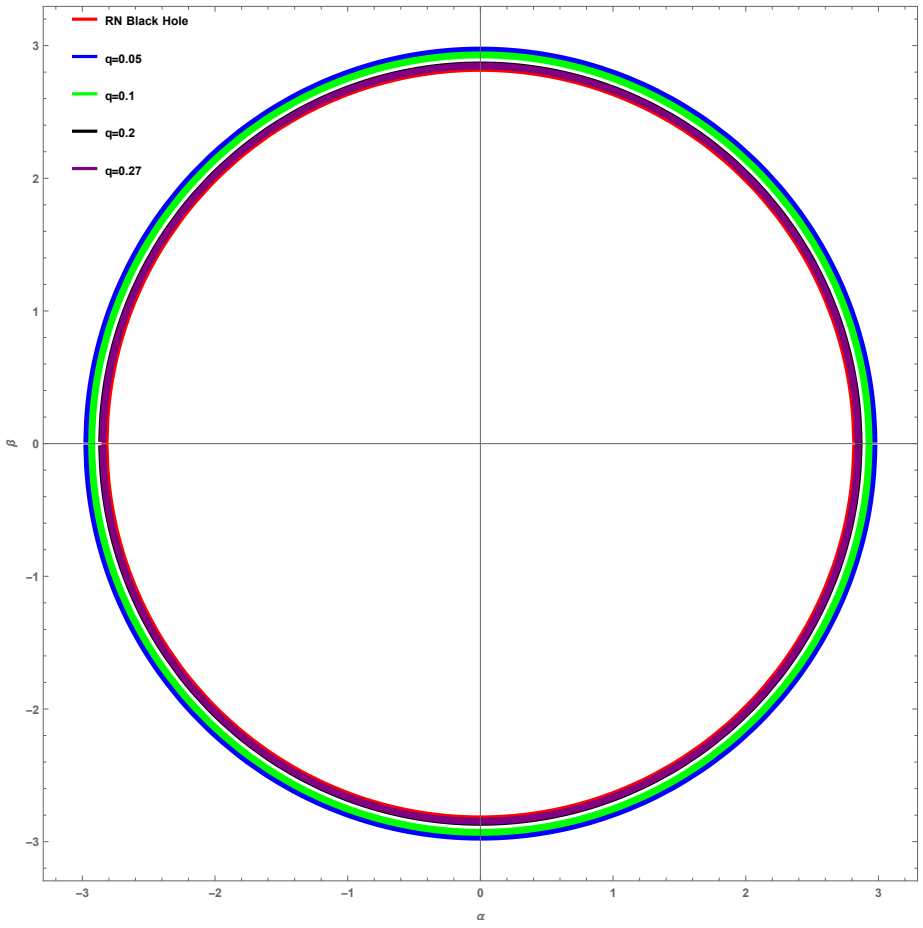

Figure 4. Shadow of the black hole for different values of q for $M_p = 1$, $M_5 = 0.5$, $M = 1$.

Here, we consider the reported angular size of the shadow of the $M87^*$ black hole by EHT as $\theta_s = (42 \pm 3)$ μas, where the distance to $M87^*$ is $D = 16.8$ Mpc, and the mass of $M87^*$ is $M = 6.5 \times 10^9$ $M_\odot$ [3]. Then, the diameter of the shadow in units of mass d_{M87^*} is given by the following [95]:

$$d_{M87^*} = \frac{D\,\theta_s}{M87^*} = 11.0 \pm 1.5. \tag{40}$$

A comparison of the radius of the shadow d_{M87} of black hole $r_{M87^*} = \frac{d_{M87^*}}{2}$ with the radius of the shadow of the tidal charged black hole R_s is shown in Table 1. It is clear that the shadow of the tidal charged black hole has a smaller radius than the shadow.

9. Effect of Plasma on Shadow of TCBH

In Ref. [76], the authors discuss in detail calculating the shadow of a spherically symmetric spacetime in a plasma medium. The line element of spherically symmetric TCBH is defined in Equation (1) as follows:

$$ds^2 = -A(r)dt^2 + \frac{dr^2}{B(r)} + r^2 d\Omega_2^2, \tag{41}$$

where

$$A(r) = [B(r)]^{-1} = 1 - \frac{2M}{M_p^2 r} + \frac{q}{M_5^2 r^2},$$

and here, we check TCBH's shadow in the presence of a plasma medium. The refractive index n can be written as follows:

$$n^2(r,\omega(r)) = 1 - \frac{\omega_e^2(r)}{\omega^2(r)}. \tag{42}$$

Here, from reference [76], we can define $h(r)$ as follows:

$$h(r)^2 = r^2\left(\frac{1}{1-\frac{2M}{M_p^2 r}+\frac{q}{M_5^2 r^2}} - \frac{\omega_e^2(r)}{\omega_\infty^2}\right). \tag{43}$$

We can calculate the radius of a photon sphere by computing the above equation as follows:

$$0 = \frac{d}{dr}\Big(h(r)^2\Big). \tag{44}$$

In this case, the value of $h(r)$ is defined by (43). We use circumstances of (44) for a photon sphere, which becomes the following:

$$0 = \frac{4r^3(r^2-\frac{2Mr}{M_p^2}+\frac{q}{M_5^2})-r^4}{\left(r^2-\frac{2Mr}{M_p^2}+\frac{q}{M_5^2}\right)^2} - 2r\frac{\omega_e^2(r)}{\omega_\infty^2} - 2r^2\frac{\omega_e(r)\omega_e(r')}{\omega_\infty^2}. \tag{45}$$

The angular radius of the shadow is defined as follows:

$$\sin^2\alpha_{sh} = \frac{h(r_{ph})^2}{h(r_O)^2}. \tag{46}$$

Now, after putting the value of Equation (43) into the Equation (46), we have the following:

$$\sin^2\alpha_{sh} = \frac{r_{ph}^2\left(\frac{1}{1-\frac{2M}{M_p^2 r_{ph}}+\frac{q}{M_5^2 r_{ph}^2}} - \frac{\omega_e^2(r_{ph})}{\omega_\infty^2}\right)}{r_O^2\left(\frac{1}{1-\frac{2M}{M_p^2 r_O}+\frac{q}{M_5^2 r_O^2}} - \frac{\omega_e^2(r_O)}{\omega_\infty^2}\right)}, \tag{47}$$

where r_{ph} has to be determined by putting Equation (43) into Equation (44). For vacuum $\omega_e(r) = 0$, our consideration gives the following:

$$h(r)^2 = r^2\left(\frac{1}{1-\frac{2M}{M_p^2 r}+\frac{q}{M_5^2 r^2}}\right) \tag{48}$$

and

$$\sin^2\alpha_{sh} = \frac{r_{ph}^2\left(\frac{1}{1-\frac{2M}{M_p^2 r_{ph}}+\frac{q}{M_5^2 r_{ph}^2}}\right)}{r_O^2\left(\frac{1}{1-\frac{2M}{M_p^2 r_O}+\frac{q}{M_5^2 r_O^2}}\right)}, \tag{49}$$

where the positive value of r_{ph} can be calculated as follows:

$$r_{ph} = \frac{1+\frac{2M}{M_p^2}+\sqrt{(1+\frac{2M}{M_p^2})^2-\frac{4q}{M_5^2}}}{2}. \tag{50}$$

10. Conclusions

In this paper, we first calculate the weak deflection angle of TCBH with the help of the Gaussian curvature. To do so, we use the GBT for calculating the weak deflection angle, which was first proposed by Gibbons and Werner. The deflection angle is found as follows:

$$\Theta \approx \frac{4M}{bM_p^2} - \frac{3q\pi}{4b^2M_5^2} + \mathcal{O}(M^2, q^2). \tag{51}$$

This shows that the weak deflection angle depends on BH's mass denoted by M, the dimensionless tidal charge denoted by q, effective Planck mass on the brane denoted by M_p, fundamental Planck scale in the 5D bulk denoted by M_5 and impact parameter b. After calculating the deflection angle of TCBH, we check its graphical behavior by varying the values of q and by fixing all the other constants. Moreover, we study the weak deflection angle of TCBH in the presence of the plasma medium, using the GBT. This angle in the presence of plasma is obtained as follows:

$$\Theta = -6\frac{M{\omega_e}^2}{b{\omega_\infty}^2{M_p}^2} - 4\frac{M}{b{M_p}^2} + 5/4\frac{q{\omega_e}^2\pi}{b^2{\omega_\infty}^2{M_5}^2} + 3/4\frac{q\pi}{b^2{M_5}^2} + \mathcal{O}(M^2, q^2, \frac{\omega_e^3}{\omega_\infty^3}). \tag{52}$$

After neglecting the plasma medium effect, we find the same angle as we find in the non-plasma case. Now if we neglect the plasma effect ($\frac{\omega_e}{\omega_\infty} \to 0$), then this deflection angle Equation (52) reduces into angle Equation (51). This shows the correctness of our angle in the presence of a plasma medium. After calculating the effect of the plasma, we find the graphical behavior of TCBH in the presence of the plasma medium. It does not show the same behavior as the behavior without the plasma. Hence, we show that the deflection angle continuously decreases with increasing q in Figures 1 and 2. Moreover, in Figure 3, we demonstrate that for increasing the value of q, decreases in the deflection angle in the plasma medium as well as the deflection angle in the plasma medium is smaller that the deflection angle in vacuum.

Last, we also find the shadow of TCBH by studying the null geodesic of TCBH. After that, we calculate the radius of the shadow and show its image in the far away observer's sky, using the celestial coordinates (α,β). Hence, we show the shadow of the black hole by changing the values of the dimensionless tidal charge q, using the constraints from the astronomical observations on the upper limiting values on the tidal charge parameters [12,14]. In Figure 4, we also discuss the radius of the shadow for positive and negative values of q. We see that the shadow's shape is a perfect circle. We conclude that for small values of q, the radius of the shadow shows a different behavior, and increasing the value of the tidal charge decreases the radius of the shadow as well as the radius of the photon sphere. Hence, we show that the shadow of the tidal-charge black hole has a smaller radius of the shadow as compared with the $M87^*$ black hole recently observed by EHT.

Author Contributions: Conceptualization, A.Ö.; Investigation, A.H. and A.Ö.; Methodology, A.Ö.; Supervision, W.J. and A.Ö.; Visualization, A.Ö.; Writing—original draft, A.H.; Writing—review & editing, A.Ö. All authors have read and agreed to the published version of the manuscript.

Funding: This research received no external funding.

Institutional Review Board Statement: Not applicable.

Informed Consent Statement: Not applicable.

Conflicts of Interest: The authors declare no conflict of interest.

References

1. Einstein, A. Lens-Like Action of a Star by the Deviation of Light in the Gravitational Field. *Science* **1936**, *84*, 506. [CrossRef] [PubMed]
2. Abbott, B.P.; Abbott, R.; Abbott, T.D.; Abernathy, M.R.; Acernese, F.; Ackley, K.; Adams, C.; Adams, T.; Addesso, P.; Adhikari, R.X.; et al. Observation of Gravitational Waves from a Binary Black Hole Merger. *Phys. Rev. Lett.* **2016**, *116*, 061102. [CrossRef] [PubMed]
3. Akiyama, K.; Antxon, A.; Alef, W.; Asada, K.; Azulay, R.; Baczko, A.-K.; Ball, D.; Baloković, M.; Barrett, J.; Bintley, D.; et al. First M87 Event Horizon Telescope Results. I. The Shadow of the Supermassive Black Hole. *Astrophys. J.* **2019**, *875*, L1.
4. Mathur, S.D. The information paradox: A pedagogical introduction. *Class. Quant. Grav.* **2009**, *26*, 224001. [CrossRef]
5. Bartelmann, M. Gravitational lensing. *Class. Quant. Grav.* **2010**, *27*, 233001. [CrossRef]
6. Keeton, C.R.; Kochanek, C.S.; Falco, E.E. The Optical Properties of Gravitational Lens Galaxies as a Probe of Galaxy Structure and Evolution. *Astrophys. J.* **1998**, *509*, 561. [CrossRef]
7. Bhadra, A. Gravitational lensing by a charged black hole of string theory. *Phys. Rev. D* **2003**, *67*, 103009. [CrossRef]
8. Whisker, R. Strong gravitational lensing by braneworld black holes. *Phys. Rev. D* **2005**, *71*, 064004. [CrossRef]
9. Chen, S.B.; Jing, J.L. Strong field gravitational lensing in the deformed Hořava-Lifshitz black hole. *Phys. Rev. D* **2009**, *80*, 024036. [CrossRef]
10. Nandi, K.K.; Zhang, Y.Z.; Zakharov, A.V. Gravitational lensing by wormholes. *Phys. Rev. D* **2006**, *74*, 024020. [CrossRef]
11. Zakharov, A.F. Constraints on a charge in the Reissner-Nordström metric for the black hole at the Galactic Center. *Phys. Rev. D* **2014**, *90*, 062007. [CrossRef]
12. Zakharov, A.F. Constraints on tidal charge of the supermassive black hole at the Galactic Center with trajectories of bright stars. *Eur. Phys. J. C* **2018**, *78*, 689. [CrossRef] [PubMed]
13. Zakharov, A.F. Constraints on a tidal charge of the supermassive black hole in M87* with the EHT observations in April 2017. *arXiv* **2021**, arXiv:2108.01533.
14. Neves, J.C.S. Constraining the tidal charge of brane black holes using their shadows. *Eur. Phys. J. C* **2020**, *80*, 717. [CrossRef]
15. Eiroa, E.F.; Romero, G.E.; Torres, D.F. Reissner-Nordström black hole lensing. *Phys. Rev. D* **2002**, *66*, 024010. [CrossRef]
16. Mao, S.; Paczynski, B. Gravitational Microlensing by Double Stars and Planetary Systems. *Astrophys. J.* **1991**, *374*, L37. [CrossRef]
17. Bozza, V. Gravitational lensing in the strong field limit. *Phys. Rev. D* **2002**, *66*, 103001. [CrossRef]
18. Hoekstra, H.; Yee, H.K.C.; Gladders, M.D. Properties of Galaxy Dark Matter Halos from Weak Lensing. *Astrophys. J.* **2004**, *606*, 67. [CrossRef]
19. Virbhadra, K.S.; Ellis, G.F.R. Gravitational lensing by naked singularities. *Phys. Rev. D* **2002**, *65*, 103004. [CrossRef]
20. Övgün, A. Black hole with confining electric potential in scalar-tensor description of regularized 4-dimensional Einstein-Gauss-Bonnet gravity. *Phys. Lett. B* **2021**, *820*, 136517. [CrossRef]
21. Virbhadra, K.S.; Ellis, G.F.R. Schwarzschild black hole lensing. *Phys. Rev. D* **2000**, *62*, 084003. [CrossRef]
22. Kasikci, O.; Deliduman, C. Gravitational lensing in Weyl gravity. *Phys. Rev. D* **2019**, *100*, 024019. [CrossRef]
23. Gallo, E.; Moreschi, O.M. Gravitational lens optical scalars in terms of energy-momentum distributions. *Phys. Rev. D* **2011**, *83*, 083007. [CrossRef]
24. Crisnejo, G.; Gallo, E. Expressions for optical scalars and deflection angle at second order in terms of curvature scalars. *Phys. Rev. D* **2018**, *97*, 084010. [CrossRef]
25. Sharif, M.; Iftikhar, S. Strong gravitational lensing in non-commutative wormholes. *Astrophys. Space Sci.* **2015**, *357*, 85. [CrossRef]
26. Gibbons, G.W. No glory in cosmic string theory. *Phys. Lett. B* **1993**, *308*, 237. [CrossRef]
27. Weinberg, S. *Gravitation and Cosmology: Principles and Applications of the General Theory of Relativity*; Wiley: New York, NY, USA, 1972.
28. Edery, A.; Paranjape, M.B. Classical tests for Weyl gravity: Deflection of light and time delay. *Phys. Rev. D* **1998**, *58*, 024011. [CrossRef]
29. Bodenner, J.; Will, C. Deflection of light to second order: A tool for illustrating principles of general relativity. *Am. J. Phys.* **2003**, *71*, 770. [CrossRef]
30. Nakajima, K.; Asada, H. Deflection angle of light in an Ellis wormhole geometry. *Phys. Rev. D* **2012**, *85*, 107501. [CrossRef]
31. Cao, W.G.; Xie, Y. Weak deflection gravitational lensing for photons coupled to Weyl tensor in a Schwarzschild black hole. *Eur. Phys. J. C* **2018**, *78*, 191. [CrossRef]
32. Wang, C.Y.; Shen, Y.F.; Xie, Y. Inflation with R^2 term in the Palatini formulation. *J. Cosmol. Astropart. Phys.* **2019**, *2019*, 022. [CrossRef]
33. Gibbons, G.W.; Werner, M.C. Applications of the Gauss–Bonnet theorem to gravitational lensing. *Class. Quantum Gravity* **2008**, *25*, 235009. [CrossRef]
34. Werner, M.C. Gravitational lensing in the Kerr-Randers optical geometry. *Gen. Rel. Grav.* **2012**, *44*, 3047–3057. [CrossRef]
35. Jusufi, K.; Sakalli, I.; Övgün, A. Effect of Lorentz symmetry breaking on the deflection of light in a cosmic string spacetime. *Phys. Rev. D* **2017**, *96*, 024040.
36. Li, Z.; Övgün, A. Finite-Distance Gravitational Deflection of Massive Particles by the Kerr-like Black Hole in the Bumblebee Gravity Model. *Phys. Rev. D* **2020**, *101*, 024040. [CrossRef]
37. Jusufi, K.; Övgün, A. Gravitational lensing by rotating wormholes. *Phys. Rev. D* **2018**, *97*, 024042. [CrossRef]

38. Kumaran, Y.; Övgün, A. Weak deflection angle of extended uncertainty principle black holes. *Chin. Phys. C* **2020**, *44*, 025101. [CrossRef]
39. Jusufi, K.; Övgün, A.; Saavedra, J.; Vasquez, Y.; Gonzalez, P.A. Deflection of light by rotating regular black holes using the Gauss-Bonnet theorem. *Phys. Rev. D* **2018**, *97*, 124024. [CrossRef]
40. Sakalli, I.; Ovgun, A. Hawking radiation and deflection of light from Rindler modified Schwarzschild black hole. *Europhys. Lett.* **2017**, *118*, 60006. [CrossRef]
41. Jusufi, K.; Övgün, A. Light Deflection by a Quantum Improved Kerr Black Hole Pierced by a Cosmic String. *Int. J. Geom. Meth. Mod. Phys.* **2019**, *16*, 1950116. [CrossRef]
42. Jusufi, K.; Övgün, A. Effect of the cosmological constant on the deflection angle by a rotating cosmic string. *Phys. Rev. D* **2018**, *97*, 064030. [CrossRef]
43. Li, Z.; He, G.; Zhou, T. Gravitational deflection of relativistic massive particles by wormholes. *Phys. Rev. D* **2020**, *101*, 044001. [CrossRef]
44. Övgün, A.; Gyulchev, G.; Jusufi, K. Weak Gravitational lensing by phantom black holes and phantom wormholes using the Gauss–Bonnet theorem. *Ann. Phys.* **2019**, *406*, 152. [CrossRef]
45. Li, Z.; Zhou, T. Equivalence of Gibbons-Werner method to geodesics method in the study of gravitational lensing. *Phys. Rev. D* **2020**, *101*, 044043. [CrossRef]
46. Jusufi, K.; Övgün, A.; Banerjee, A.; Sakalli, I. Gravitational lensing by wormholes supported by electromagnetic, scalar, and quantum effects. *Eur. Phys. J. Plus* **2019**, *134*, 428. [CrossRef]
47. Li, Z.; Jia, J. The finite-distance gravitational deflection of massive particles in stationary spacetime: A Jacobi metric approach. *Eur. Phys. J. C* **2020**, *80*, 157. [CrossRef]
48. Jusufi, K.; Werner, M.C.; Banerjee, A.; Övgün, A. Light deflection by a rotating global monopole spacetime. *Phys. Rev. D* **2017**, *95*, 104012. [CrossRef]
49. Takizawa, K.; Ono, T.; Asada, H. Gravitational deflection angle of light: Definition by an observer and its application to an asymptotically nonflat spacetime. *Phys. Rev. D* **2020**, *101*, 104032. [CrossRef]
50. Ono, T.; Ishihara, A.; Asada, H. Deflection angle of light for an observer and source at finite distance from a rotating global monopole. *Phys. Rev. D* **2019**, *99*,124030. [CrossRef]
51. Ono, T.; Ishihara, A.; Asada, H. Deflection angle of light for an observer and source at finite distance from a rotating wormhole. *Phys. Rev. D* **2018**, *98*, 044047. [CrossRef]
52. Ono, T.; Asada, H. The effects of finite distance on the gravitational deflection angle of light. *Universe* **2019**, *5*, 218. [CrossRef]
53. Pantig, R.C.; Rodulfo, E.T. Weak lensing of a dirty black hole. *Chin. J. Phys.* **2020**, *66*, 691–702. [CrossRef]
54. Övgün, A.; Jusufi, K.; Sakalli, I. Gravitational lensing under the effect of Weyl and bumblebee gravities: Applications of Gauss–Bonnet theorem. *Ann. Phys.* **2018**, *399*, 193. [CrossRef]
55. Övgün, A.; Jusufi, K.; Sakalli, I. Exact traversable wormhole solution in bumblebee gravity. *Phys. Rev. D* **2019**, *99*, 024042. [CrossRef]
56. Övgün, A.; Sakalli, I.; Saavedra, J. Shadow cast and Deflection angle of Kerr-Newman-Kasuya spacetime. *JCAP* **2018**, *1810*, 041. [CrossRef]
57. Övgün, A. Deflection Angle of photons through dark matter by black holes and wormholes using Gauss–Bonnet theorem. *Universe* **2019**, *5*, 115. [CrossRef]
58. Övgün, A. Light deflection by Damour-Solodukhin wormholes and Gauss-Bonnet theorem. *Phys. Rev. D* **2018**, *98*, 044033. [CrossRef]
59. Övgün, A.; Sakalli, I.; Saavedra, J. Weak gravitational lensing by Kerr-MOG black hole and Gauss–Bonnet theorem. *Ann. Phys.* **2019**, *411*, 167978. [CrossRef]
60. Övgün, A. Weak field deflection angle by regular black holes with cosmic strings using the Gauss-Bonnet theorem. *Phys. Rev. D* **2019**, *99*, 104075. [CrossRef]
61. Javed, W.; Babar, R.; Övgün, A. Effect of the Brane-Dicke coupling parameter on weak gravitational lensing by wormholes and naked singularities. *Phys. Rev. D* **2019**, *99*, 084012 [CrossRef]
62. Javed, W.; Babar, R.; Övgün, A. Effect of the dilaton field and plasma medium on deflection angle by black holes in Einstein-Maxwell-dilaton-axion theory. *Phys. Rev. D* **2019**, *100*, 104032. [CrossRef]
63. Javed, W.; Abbas, J.; Övgün, A. Effect of the hair on deflection angle by asymptotically flat black holes in Einstein-Maxwell-dilaton theory. *Phys. Rev. D* **2019**, *100*, 044052. [CrossRef]
64. Javed, W.; Abbas, J.; Övgün, A. Deflection angle of photon from magnetized black hole and effect of nonlinear electrodynamics. *Eur. Phys. J. C* **2019**, *79*, 694. [CrossRef]
65. Javed, W.; Khadim, M.B.; Övgün, A.; Abbas, J. Weak gravitational lensing by stringy black holes. *Eur. Phys. J. Plus* **2020**, *135*, 314. [CrossRef]
66. Ishihara, A.; Suzuki, Y.; Ono, T.; Kitamura, T.; Asada, H. Gravitational bending angle of light for finite distance and the Gauss-Bonnet theorem. *Phys. Rev. D* **2016**, *94*, 084015. [CrossRef]
67. Ono, T.; Ishihara, A.; Asada, H. Gravitomagnetic bending angle of light with finite-distance corrections in stationary axisymmetric spacetimes. *Phys. Rev. D* **2017**, *96*, 104037. [CrossRef]

68. Ishihara, A.; Suzuki, Y.; Ono, T.; Asada, H. Finite-distance corrections to the gravitational bending angle of light in the strong deflection limit. *Phys. Rev. D* **2017**, *95*, 044017. [CrossRef]
69. Crisnejo, G.; Gallo, E. Weak lensing in a plasma medium and gravitational deflection of massive particles using the Gauss-Bonnet theorem. A unified treatment. *Phys. Rev. D* **2018**, *97*, 124016. [CrossRef]
70. Bisnovatyi-Kogan, G.S.; Tsupko, O.Y. Gravitational radiospectrometer. *Gravit. Cosmol.* **2009**, *15*, 20. [CrossRef]
71. Okyay, M.; Övgün, A. Nonlinear electrodynamics effects on the black hole shadow, deflection angle, quasinormal modes and greybody factors. *arXiv* **2021**, arXiv:2108.07766.
72. Bisnovatyi-Kogan, G.S.; Tsupko, O.Y. Gravitational lensing in a non-uniform plasma. *Mon. Not. R. Astron. Soc.* **2010**, *404*, 1790. [CrossRef]
73. Tsupko, O.Y.; Bisnovatyi-Kogan, G.S. Gravitational lensing in plasma: Relativistic images at homogeneous plasma. *Phys. Rev. D* **2013**, *87*, 124009. [CrossRef]
74. Tsupko, O.Y.; Bisnovatyi-Kogan, G.S. Influence of plasma on relativistic images of gravitational lensing. *Nonlin. Phenom. Complex Syst.* **2014**, *17*, 455.
75. Tsupko, O.Y.; Bisnovatyi-Kogan, G.S. Gravitational lensing in the presence of plasmas and strong gravitational fields. *Gravit. Cosmol.* **2014**, *20*, 220. [CrossRef]
76. Perlick, V.; Tsupko, O.Y.; Bisnovatyi-Kogan, G.S. Influence of a plasma on the shadow of a spherically symmetric black hole. *Phys. Rev. D* **2015**, *92*, 104031.
77. Bisnovatyi-Kogan, G.S.; Tsupko, O.Y. Gravitational lensing in plasmic medium. *Plasma Phys. Rep.* **2015**, *41*, 562. [CrossRef]
78. Pantig, R.C.; Rodulfo, E.T. Rotating dirty black hole and its shadow. *Chin. J. Phys.* **2020**, *68*, 236–257. [CrossRef]
79. Perlick, V.; Tsupko, O.Y. Light propagation in a plasma on Kerr spacetime: Separation of the Hamilton-Jacobi equation and calculation of the shadow. *Phys. Rev. D* **2017**, *95*, 104003. [CrossRef]
80. Bisnovatyi-Kogan, G.; Tsupko, O. Gravitational lensing in presence of Plasma: Strong lens systems, black hole lensing and shadow. *Universe* **2017**, *3*, 57. [CrossRef]
81. Morozova, V.S.; Ahmedov, B.J.; Tursunov, A.A. Gravitational lensing by a rotating massive object in a plasma. *Astrophys. Space Sci.* **2013**, *346*, 513. [CrossRef]
82. Abdujabbarov, A.; Juraev, B.; Ahmedov, B.; Stuchlik, Z. Shadow of rotating wormhole in plasma environment. *Astrophys. Space Sci.* **2016**, *361*, 226. [CrossRef]
83. Abdujabbarov, A.; Toshmatov, B.; Stuchlik, Z.; Ahmedov, B. Shadow of the rotating black hole with quintessential energy in the presence of plasma. *Int. J. Mod. Phys. Conf. Ser.* **2017**, *26*, 1750051. [CrossRef]
84. Abdujabbarov, A.; Toshmatov, B.; Schee, J.; Stuchlik, Z.; Ahmedov, B. Gravitational lensing by regular black holes surrounded by plasma. *Int. J. Mod. Phys. D* **2017**, *26*, 1741011. [CrossRef]
85. AAbdujabbarov; Ahmedov, B.; Dadhich, N.; Atamurotov, F. Optical properties of a braneworld black hole: Gravitational lensing and retrolensing. *Phys. Rev. D* **2017**, *96*, 084017. [CrossRef]
86. Turimov, B.; Ahmedov, B.; Abdujabbarov, A.; Bambi, C. Gravitational lensing by a magnetized compact object in the presence of plasma. *Int. J. Mod. Phys. D* **2019**, *28*, 2040013. [CrossRef]
87. Rogers, A. Frequency-dependent effects of gravitational lensing within plasma. *Mon. Not. R. Astron. Soc.* **2015**, *451*, 17. [CrossRef]
88. Rogers, A. Escape and trapping of low-frequency gravitationally lensed rays by compact objects within plasma. *Mon. Not. R. Astron. Soc.* **2017**, *465*, 2151. [CrossRef]
89. Rogers, A. Gravitational lensing of rays through the levitating atmospheres of compact objects. *Universe* **2017**, *3*, 3. [CrossRef]
90. Er, X.; Rogers, A. Two families of astrophysical diverging lens models. *Mon. Not. R. Astron. Soc.* **2018**, *475*, 867. [CrossRef]
91. Kocherlakota, P.; Rezzolla, L.; Falcke, H.; Fromm, C.M.; Kramer, M.; Mizuno, Y.; Nathanail, A.; Olivares, H.; Younsi, Z.; Akiyama, K.; et al. Constraints on black-hole charges with the 2017 EHT observations of M87*. *Phys. Rev. D* **2021**, *103*, 104047. [CrossRef]
92. Konoplya, R.A.; Pappas, T.; Zhidenko, A. Einstein-scalar-Gauss-Bonnet black holes: Analytical approximation for the metric and applications to calculations of shadows. *Phys. Rev. D* **2020**, *101*, 044054. [CrossRef]
93. Konoplya, R.A. Shadow of a black hole surrounded by dark matter. *Phys. Lett. B* **2019**, *795*, 1. [CrossRef]
94. Lu, X.; Xie, Y. Weak and strong deflection gravitational lensing by a renormalization group improved Schwarzschild black hole. *Eur. Phys. J. C* **2019**, *79*, 1016. [CrossRef]
95. Allahyari, A.; Khodadi, M.; Vagnozzi, S.; Mota, D.F. Magnetically charged black holes from non-linear electrodynamics and the Event Horizon Telescope. *JCAP* **2002**, *2020*, 003. [CrossRef]
96. Narayan, R.; Johnson, M.D.; Gammie, C.F. The Shadow of a Spherically Accreting Black Hole. *Astrophys. J.* **2019**, *885*, L33. [CrossRef]
97. Ding, C.; Liu, C.; Casana, R.; Cavalcante, A. Exact Kerr-like solution and its shadow in a gravity model with spontaneous Lorentz symmetry breaking. *Eur. Phys. J. C* **2020**, *80*, 178. [CrossRef]
98. Shaikh, R.; Joshi, P.S. Can we distinguish black holes from naked singularities by the images of their accretion disks? *JCAP* **2019**, *1910*, 064. [CrossRef]
99. Banerjee, I.; Chakraborty, S.; SenGupta, S. Silhouette of M87*: A New Window to Peek into the World of Hidden Dimensions. *Phys. Rev. D* **2020**, *101*, 041301. [CrossRef]
100. Carter, B. Global structure of the Kerr family of gravitational fields. *Phys. Rev.* **1968**, *174*, 1559. [CrossRef]

101. Bardeen, J. Black holes. In *Proceeding of the Les Houches Summer School, Session 215239*; Cécile DeWitt and Bryce DeWitt; Gordon and Breach: New York, NY, USA, 1973.
102. Chandrasekhar, S. *The Mathematical Theory of Black Holes*; Oxford University Press: New York, NY, USA, 1992.
103. Dadhich, N.; Maartens, R.; Papadopoulos, P.; Rezania, V. Black holes on the brane. *Phys. Lett. B* **2000**, *487*, 1. [CrossRef]
104. Pradhan, P. Circular Geodesics in Tidal Charged Black Hole. *Int. J. Geom. Meth. Mod. Phys.* **2017**, *15*, 1850011. [CrossRef]
105. Keeton, C.R. and Petters, A.O. Formalism for testing theories of gravity using lensing by compact objects: Static, spherically symmetric case. *Phys. Rev. D* **2005**, *72*, 104006. [CrossRef]
106. Synge, J.L. The Escape of Photons from Gravitationally Intense Stars. *Mon. Not. R. Astron. Soc.* **1966**, *131*, 463. [CrossRef]